



Studies on the Syntheses, Characterization, Docking-, DFT Analysis, Antimicrobial-, DNA Cleaving-, and Antituberculosis Screening of Tricyclic Pyrazole Derivatives

P. Palanisamy¹, R. Subramanian², S. Nalini³, S. Kumaresan^{4*}

¹Department of Chemistry, Pioneer Kumaraswamy College, Nagercoil-629003, TN, India

²Centre for Scientific and Applied Research, PSN College of Engineering and Technology, Melathediyoor, Tirunelveli-627 152, TN, India

³Department of Chemistry, Manonmaniam Sundaranar University, Tirunelveli-627 012, TN, India

^{4*}Department of Biotechnology, Manonmaniam Sundaranar University, Tirunelveli-627 012, TN, India

Received: 07-02-2016 / Revised: 21-02-2016 / Accepted: 27-02-2016 / Published: 28-02-2016

Abstract

Six pyrazole derivatives have been synthesized from the key-intermediates 2,3-dihydrothiochromen-4-one and 3,4-dihydrobenzo[b]thiepin-5(2H)-one. These compounds have been characterized by IR, ¹H-NMR, ¹³C-NMR, Mass, and CHN analysis. These are subjected to antimicrobial-, antituberculosis-, and DNA cleaving studies. The docking patterns for the pyrazole derivatives with 1M17 protein have been studied. DFT calculations were performed using Gaussian 09 software. Compound **6** has a lower binding energy (-218.45 Kcal/mol) and showed the highest antimicrobial- and antituberculosis activity. Chlorine-substituted pyrazole derivatives (**5**, **6**, **9**, and **10**) completely cleaved the DNA compared to their nitro-substituted counterparts.

Key words: Tricyclicpyrazole, antimicrobial-, antituberculosis-, DNA cleaving, DFT studies

INTRODUCTION

Pyrazoles and their analogous have attracted much attention due to various biological activities [1, 2]. These derivatives exhibit significant properties such as antitumor, anti-HIV, anti-inflammatory, and anti-microbial agents [3]. Continuous interest is focused on the synthesis of C₂-substituted thiazolidinone derivatives due to their broad spectrum biological activities like antibacterial-, antituberculosis-, antifungal-, and anticancer activity [4-9]. Pyrazole and its derivatives are used as antipyretics, antirheumatoid agents, herbicides, fungicides, metal ion extracts [10, 11], and corrosion inhibitors [12]. They display an important role in the preparation of biologically active molecules [13, 14] with several applications as analgesics, anti-inflammatory-, antibacterial-, and anti-depressive agents [15-17]. Addition of a substituent group in pyrazole moiety leads to variation of charge distribution in the molecules which consequently affects the structural-, electronic-, and vibrational parameters. Methyl and amino groups are generally noticed as electron donating substituents in aromatic ring systems [18]. The azole group of heterocyclic compounds

exhibits significant lipophilicity that influences the ability of drug to reach the target by transmembrane diffusion, showing resistance against TB [19, 20]. It has been known that compounds containing pharmacophores such as CNNC display several bioactivity [20a].

In view of the above noticed facts and in continuation of our interest in the synthesis of sulphur-containing heterocycles [21-23], we report herein the syntheses, characterization, docking-, DFT analysis, antimicrobial-, DNA cleaving-, and antituberculosis screening of some tricyclic pyrazole derivatives incorporating thiochromeno- and benzothiepine moieties.

EXPERIMENTAL

General comments: FT IR spectra were recorded on a JASCO FT-IR Model 410 spectrophotometer. The recording was performed in the 4000-400 cm⁻¹ wave number range. All NMR spectra were taken on a Bruker Advance 400 FT-NMR spectrometer with ¹H observed at 400 MHz and ¹³C observed at 400 MHz. Chemical shifts for ¹H and ¹³C-NMR spectra were reported in δ or ppm downfield from

*Corresponding Author Address: Dr. S. Kumaresan, Professor of Chemistry (Emeritus-UGC) Department of Biotechnology, Manonmaniam Sundaranar University, Tirunelveli-627 012, Tamilnadu, India; E-mail: skumarmsu@yahoo.com

TMS [(CH₃)₄Si]. ESI mass spectra were obtained on an Agilent 6520 ES+2000 spectrometer. All chemicals were purchased commercially and used as such. Each set of reaction was monitored using TLC plates prepared from silica gel (Merck) grade. The products formed were purified by column chromatography using silica gel, 60-120 mesh (Merck).

Synthesis:

Synthesis of 3-(4-chlorophenyl)-2,3,3a,4-tetrahydro-2-phenylthiochromeno[4,3-c]pyrazole (5)

Compound 5 was obtained as a colourless solid (0.61g, 56%). Rf = 0.62 (petroleum ether/EtOAc, 8:2); mp 245-248 °C; The IR (KBr) 1583, 1283, 1199, and 1083 cm⁻¹. ¹H-NMR (CDCl₃) δ 2.4 ppm (1H, m, CH-CH-CH₂), 2.9 (2H, d, CH-CH-CH₂), 3.9 (1H, d, CH-CH-CH₂), and 6.8-7.5 ppm (13H, aromatic protons). ¹³C-NMR (CDCl₃) 29.6, 49.5, 54.2, 113.5, 117.3, 125.6, 126.9, 129.5, 129.6, 129.7, 131.4, 138.2, 141.4, 143.7, and 150.9. Mass m/z: 376.02 and Anal. Calcd for C₂₂H₁₇ClN₂S; C, 70.11; H, 4.55; N, 9.41; S, 8.51, Found: C, 70.01; H, 4.23; N, 7.25; S, 8.31%.

Synthesis of 3-(4-chlorophenyl)-2-phenyl-3,3a,4,5-tetrahydro-2H-[1]benzothiepin[5,4-c]pyrazole (6)

Compound 6 was got as a colourless solid (0.63g, 58%). Rf = 0.64 (petroleum ether/EtOAc, 8:2); mp 253-256 °C; IR (KBr) 1603, 1305, 1206, and 1104 cm⁻¹. ¹H-NMR (CDCl₃) δ 1.8 (2H, m, S-CH₂-CH₂) and 2.1 (1H, m, CH₂-CH₂-CH), δ 2.9 (2H, t, S-CH₂-CH₂), 3.9 (1H, d, CH₂-CH-CH), and 6.8-7.6 ppm (13H, aromatic protons). ¹³C-NMR (CDCl₃) 26.4, 26.5, 36.1, 53.6, 55.6, 113.5, 117.2, 121.6, 128.4, 129.3, 129.4, 129.6, 130.2, 138.6, 140.5, 143.5, and 151.4. Mass m/z 390.09 and Anal. Calcd for C₂₃H₁₉ClN₂S; C, 70.66; H, 4.90; N, 7.17; S, 8.20, Found: C, 70.52; H, 4.76; N, 7.01; S, 8.03.

Synthesis of 3-(2-chlorophenyl)-2,3,3a,4-tetrahydro-2-phenylthiochromeno[4,3-c]pyrazole (9)

Compound 9 was obtained as a colorless solid (0.51g, 53%). Rf = 0.58 (petroleum ether/EtOAc, 8:2); mp 243-246 °C; IR (KBr) 1576, 1293, 1206, and 1068 cm⁻¹. ¹H-NMR (CDCl₃) δ 2.5 (1H, m, CH-CH-CH₂), 2.8 (2H, d, CH-CH-CH₂), 3.9 (1H, d, CH-CH-CH₂), and 6.9-7.6 ppm (13H, aromatic protons). ¹³C-NMR (CDCl₃) 29.5, 49.6, 54.1, 113.5, 117.5, 125.4, 126.2, 129.3, 129.5, 129.2, 131.6, 138.3, 141.2, 143.2, and 151.2. Mass m/z: 376.04 and Anal. Calcd for C₂₂H₁₇ClN₂S; C, 70.11; H, 4.55; N, 7.43; S, 8.51, Found: C, 70.11; H, 4.19; N, 7.21; S, 8.29%.

Synthesis of 3-(2-chlorophenyl)-2-phenyl-3,3a,4,5-tetrahydro-2H-[1]benzothiepin[5,4-c]pyrazole (10)

Compound 10 was got as a colorless solid (0.51g, 53%). Rf = 0.58 (petroleum ether/EtOAc, 8:2); mp 252-255 °C; IR (KBr) spectrum 1608, 1301, 1208, and 1112 cm⁻¹. ¹H-NMR (CDCl₃) δ 1.7 ppm (2H, m, S-CH₂-CH₂), 2.0 (1H, m, CH₂-CH₂-CH), 2.8 (2H, t, S-CH₂-CH₂), 3.8 (1H, d, CH₂-CH-CH), and 6.5-7.6 ppm (13H, aromatic protons). ¹³C-NMR (CDCl₃) 26.8, 26.2, 36.3, 53.5, 55.2, 113.6, 117.1, 121.4, 128.5, 129.1, 129.5, 129.5, 130.2, 138.3, 140.4, 143.5, and 151.9. Mass m/z 390.05 and Anal. Calcd for C₂₃H₁₉ClN₂S; C, 70.66; H, 4.90; N, 7.17; S, 8.20, Found: C, 70.42; H, 4.66; N, 7.12, S, 8.14.

Synthesis of 3-(4-nitrophenyl)-2,3,3a,4-tetrahydro-2-phenylthiochromeno[4,3-c]pyrazole (13)

Compound 13 was obtained as a colorless solid (0.51g, 53%). Rf = 0.58 (petroleum ether/EtOAc, 8:2); mp 265-268 °C; IR (KBr) 1598, 1311, 1214, and 1116 cm⁻¹. ¹H-NMR (CDCl₃) δ 2.5 (1H, m, CH-CH-CH₂), 2.9 (2H, d, CH-CH-CH₂), 3.8 (1H, d, CH-CH-CH₂), 7.7-8.2 ppm (13H, aromatic protons). ¹³C-NMR (CDCl₃) 29.6, 49.3, 53.6, 113.5, 117.6, 121.5, 129.2, 129.3, 129.4, 141.5, 143.5, 145.6 and 151.4. Mass m/z 387.10 and Anal. Calcd for C₂₂H₁₇N₃O₂S; C, 68.20; H, 4.42; N, 10.85; S, 8.28, Found: C, 68.09; H, 4.32; N, 10.71; S, 8.09.

Synthesis of 3-(4-nitrophenyl)-2-phenyl-3,3a,4,5-tetrahydro-2H-[1]benzothiepin[5,4-c]pyrazole (14)

Compound 14 was got as a colorless solid (0.51g, 53%). Rf = 0.58 (petroleum ether/EtOAc, 8:2); mp 271-273 °C; IR (KBr) 1603, 1305, 1206, and 1104 cm⁻¹. δ 1.9 (2H, m, S-CH₂-CH₂), 2.2 (1H, m, CH₂-CH₂-CH), 3.0 (2H, t, S-CH₂-CH₂), 4.0 (1H, d, CH₂-CH-CH), and 7.2-7.7 ppm (13H, aromatic protons). ¹³C-NMR (CDCl₃) 27.5, 33.5, 52.4, 54.9, 113.3, 117.3, 120.5, 129.5, 129.8, 141.6, 143.3, 145.3 and 151.9. Mass m/z 410.12 and Anal. Calcd for C₂₃H₁₉N₃O₂S; C, 68.81; H, 4.77; N, 10.47; S, 7.99, Found: C, 68.72; H, 4.70; N, 10.39; S, 7.90.

Molecular docking study: Docking calculations of all synthesized compounds (**5**, **6**, **9**, **10**, **13**, and **14**) were carried out using Docking Server. The MMFF94 force field was used for energy minimization of ligand molecule using Docking Server. Gasteiger partial charges were added to the ligand atoms. Docking calculations were carried out on *IM17* protein model. Essential hydrogen atoms, Kollman united atom type charges, and solvation parameters were added with the aid of AutoDock tools. Affinity (grid) maps of 20×20×20 Å grid points and 0.375 Å spacing were generated using the Autogrid program [37]. AutoDock parameter set- and distance-dependent dielectric

functions were used in the calculation of the van der Waals and the electrostatic terms respectively.

DFT study: The theoretical energy calculation of the synthesized compounds **5**, **6**, **9**, **10**, **13**, and **14** in gas phase was performed using the analytical gradient methods of DFT with Becke's three parameters (B3) exchange functional together with the Lee–Yang–Parr (LYP) non-local correlation functional, symbolized B3LYP by means of 3-21G (d,p) basis set implemented in Gaussian 09 software package [33].

Antimicrobial evaluation: Standard sterilized filter paper discs (5 mm diameter) impregnated with a solution of the test compound in DMSO (1 mg/mL) was placed on an agar plate seeded with the appropriate test organism in triplicates. Gram-positive bacteria, *Staphylococcus aureus*, *Streptococcus pneumoniae*, and *Klebsiella pneumoniae* as well as Gram-negative bacteria, *Pseudomonas aeruginosa*, and *Escherichia coli* were used. They were also evaluated for their *in vitro* antifungal potential against *Candida albicans*, *Aspergillus flavus*, and *Aspergillus niger* strains. Ampicillin was used both as a standard antibacterial agent and antifungal agent. DMSO alone was used as control at the above-mentioned concentration. The plates were incubated at 37 °C for 24h for bacteria and 28 °C and 48h for fungi.

Antituberculosis activity: All the compounds were screened for their *in vitro* antituberculosis activity against MTB using the resazurin microplate assay (REMA) [38, 39]. MTB H₃₇Rv was grown in Middlebrook 7H11 broth medium supplemented with 10% OADC (oleic acid, albumin, dextrose, and catalase; 1, 10, 100 µg /L). After incubation at 37 °C for 7 days, 15 µL of 0.01% resazurin (Sigma, St. Louis, MO, USA) solution in sterile water was added to the first growth control wells and incubated for 24h. When the first set of growth controls turned pink, the dye solution was added to the second set of growth controls and the test wells, and incubated for 24h at 37 °C. Blue color in the wells containing the test compounds would indicate inhibition of growth and pink would indicate lack of inhibition of growth of *M. tuberculosis*. The minimum inhibitory concentration (MIC) is defined as the minimum concentration of compound required to 99.9% inhibition of bacterial growth.

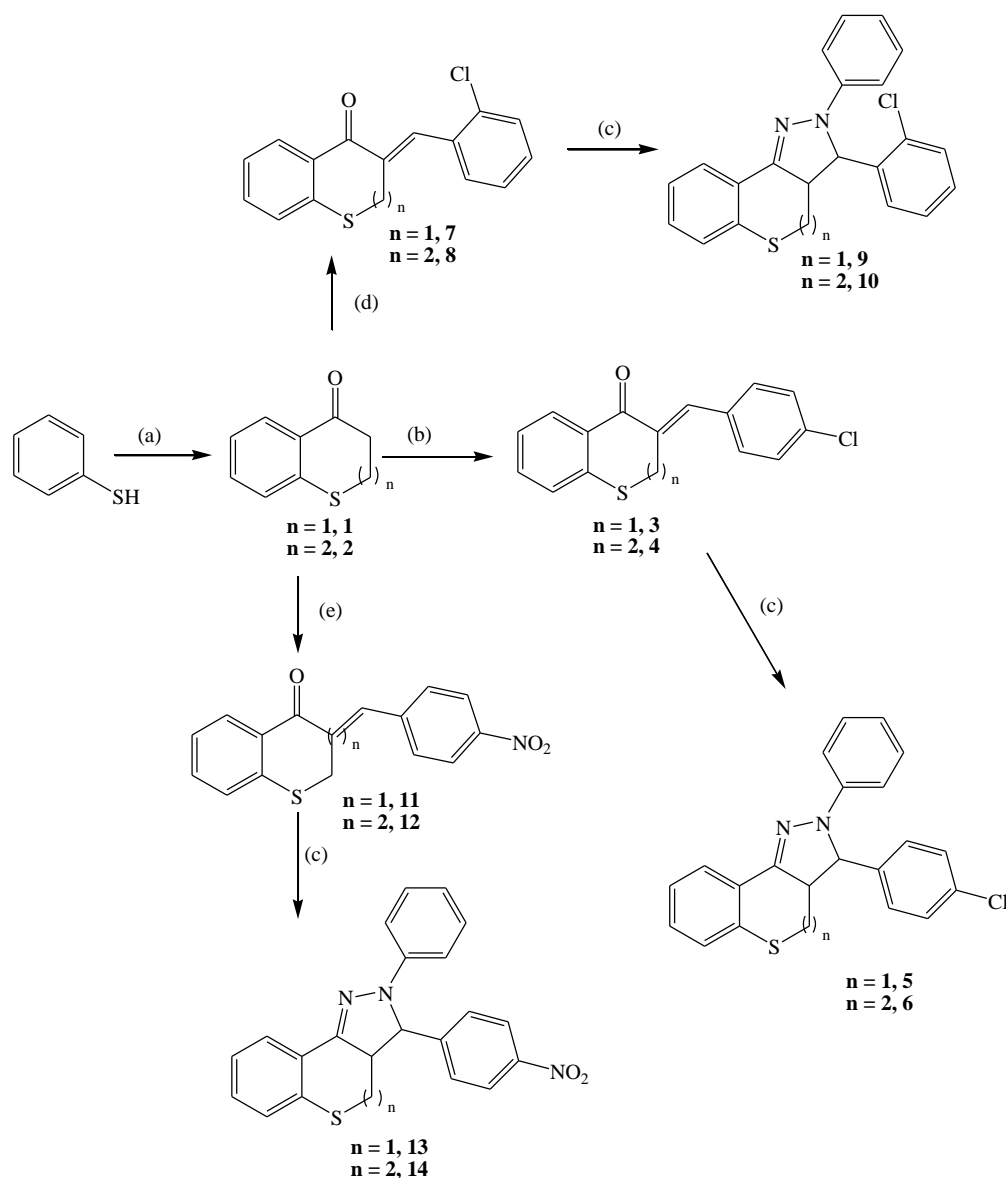
DNA cleavage: For investigation of the DNA cleavage potential of the tricyclic pyrazole

compounds **5**, **6**, **9**, **10**, **13**, and **14**, *E. coli* was used as the test candidate. Electrophoresis sample solutions were prepared by 4.0 µL of the solution (prepared by dissolving of 5 mg of each compound in 1 mL DMSO) and 4.0 µL DNA. The samples were incubated at 37 °C for 2h. After incubation, the samples were mixed with bromophenol blue dye and then were carefully loaded into the wells along with the standard DNA (alone), the DNA-H₂O₂ mixture. Gel electrophoresis performance on the samples was carried out at constant 100 V of electricity for about 30 min. The resultant bands of electrophoresis were visualized by UV light and then photographed [40].

RESULTS AND DISCUSSION

Chemistry: The synthetic sequence for the pyrazole derivatives **5**, **6**, **9**, **10**, **13**, and **14** is summarized in Scheme 1. In the initial step, 2,3-dihydrothiochromen-4-one/3,4-dihydrobenzo[b]thiepin-5(2H)-one and appropriate aromatic aldehydes in ethanolic sodium hydroxide solution were stirred at room temperature giving the Claisen-Schmidt condensation products **3**, **4**, **7**, **8**, **11**, and **12**. These products were treated with phenylhydrazine hydrochloride to furnish the pyrazole derivatives. The yields of the pyrazole derivatives were ranging from 66-68% after recrystallization with absolute ethanol. The purity of the compounds was monitored by TLC using the ethyl acetate:hexane (9:1) elutant followed by elemental analyses. Both the analytical and spectral data of all the synthesized compounds were in full accordance with the proposed structures.

The IR (KBr) spectra of compounds **5**, **6**, **9**, **10**, **13**, and **14** displayed the pyrazoline C=N_{str} in the region 1576-1608 cm⁻¹, Ar-N_{str} in 1283-1311 cm⁻¹, N-N-C_{str} in region 1576-1608 cm⁻¹, and C-N_{str} 1068-1116 cm⁻¹. The ¹H-NMR (CDCl₃) spectrum of **5** displayed a multiplet at δ 2.4 ppm (1H, m, CH-CH-CH₂), two doublets at δ 2.9 (2H, d, CH-CH-CH₂) and δ 3.9 (1H, d, CH-CH-CH₂), and a multiplet in the region δ 6.8-7.5 ppm (13H, aromatic protons). The C=N absorbs at 151.06 ppm in the ¹³C-NMR. The ¹H-NMR (CDCl₃) spectrum of **6** showed two multiplets at δ 1.8 ppm (2H, m, S-CH₂-CH₂) and 2.1 (1H, m, CH₂-CH₂-CH), a triplet at δ 2.9 (2H, t, S-CH₂-CH₂), a doublet at δ 3.9 (1H, d, CH-CH-CH₂), and a multiplet at δ 6.8-7.6 ppm (13H, aromatic protons). The C=N absorbs at 150.76 ppm in the ¹³C-NMR.



Scheme 1: Protocol for the synthesis of pyrazole derivatives based on thiochromeno- and benzothiepieno moieties. Reaction and conditions: (a) $\text{ClCH}_2\text{COOH}/\text{NaOH}/\text{PPA}$ or $\text{ClCH}_2\text{CH}_2\text{COOH}/\text{NaOH}/\text{PPA}$ (b) Na, dry EtOH, p-chlorobenzaldehyde (c) $\text{C}_6\text{H}_5\text{NHNH}_2\cdot\text{HCl}$, CH_3COOH (d) Na, dry EtOH, o-chlorobenzaldehyde (e) Na, dry EtOH, p-nitrobenzaldehyde

The $^1\text{H-NMR}$ (CDCl_3) spectrum of **9** showed a multiplet at δ 2.5 ppm (1H, m, CH-CH_2), two doublets at δ 2.8 (2H, d, CH-CH_2) and δ 3.9 (1H, d, CH-CH_2), and a multiplet in the region δ 6.9-7.6 ppm (13H, aromatic protons). The C=N registers at 151.56 ppm in the $^{13}\text{C-NMR}$. The $^1\text{H-NMR}$ (CDCl_3) spectrum of **10** showed two multiplets at δ 1.7 ppm (2H, m, S-CH_2) and 2.0 (1H, m, CH_2), a triplet at δ 2.8 (2H, t, S-CH_2), a doublet at δ 3.8 (1H, d, CH_2), and a multiplet at δ 6.5-7.6 ppm (13H, aromatic protons). The C=N absorbs at 150.96 ppm in the $^{13}\text{C-NMR}$. The $^1\text{H-NMR}$ (CDCl_3) spectrum

of **13** displayed a multiplet at δ 2.5 ppm (1H, m, CH-CH_2), two doublets at δ 2.9 (2H, d, CH-CH_2) and δ 3.8 (1H, d, CH-CH_2), and a multiplet in the region δ 7.7-8.2 ppm (13H, aromatic protons). The C=N absorbs in the region 151.16 ppm in the $^{13}\text{C-NMR}$. The $^1\text{H-NMR}$ (CDCl_3) spectrum of **14** showed a two multiplets at δ 1.9 ppm (2H, m, S-CH_2) and 2.2 (1H, m, CH_2), a triplet at δ 3.0 (2H, t, S-CH_2), a doublet at δ 4.0 (1H, d, CH_2), and a multiplet in the region δ 7.2-7.7 ppm (13H, aromatic protons). The C=N absorbs at 150.23 ppm in the $^{13}\text{C-NMR}$.

Docking studies of compounds 5, 6, 9, 10, 13, and 14 on 1M17 protein: 'AutoDock Tools' (ADT) is useful to generate grids, calculate the dock score and evaluate the conformers [24]. From the docking results, the best scoring (*i.e.* with the lowest docking energy) docked model of a compound is chosen to represent its most possible binding mode [25]. From these results, the

molecules are represented as active, moderately active, or inactive [26]. Docking calculations were carried out using docking server [27]. The MMFF94 force field [28] was used for energy minimization of the ligand molecules using the docking server. Gasteiger partial charges were added to the ligand atoms. Non-polar hydrogen atoms were merged and rotatable bonds were defined.



Fig. 1. Structure of 1M17 protein

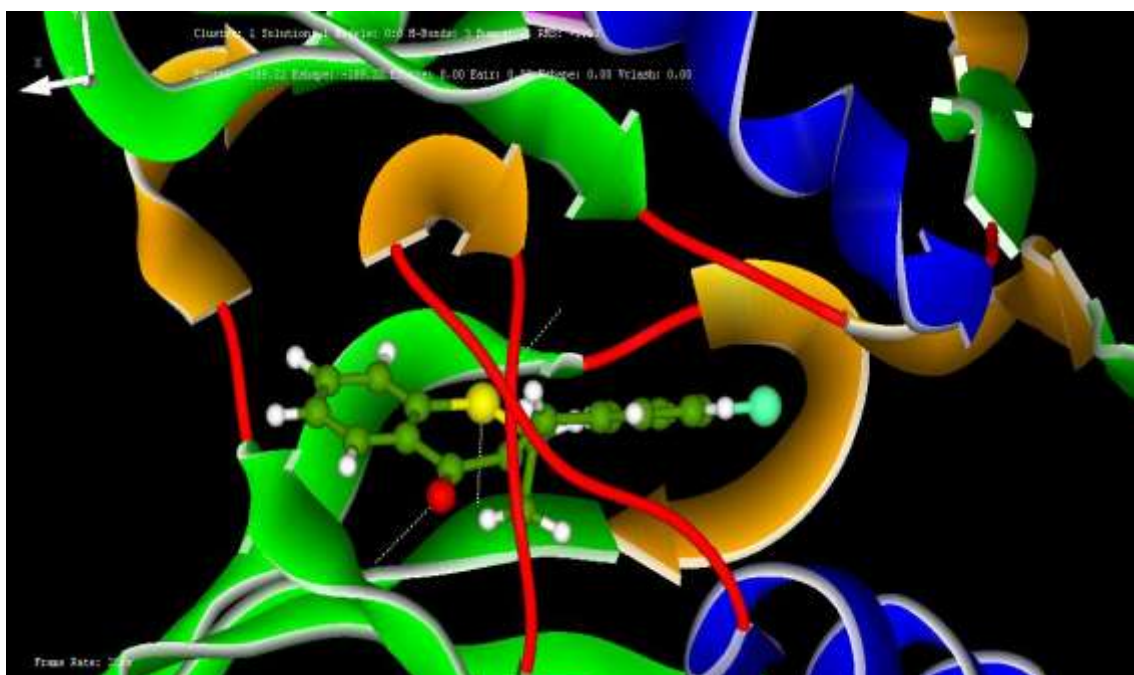


Fig. 2. Docking pose of 3-(4-chlorophenyl)-2,3,3a,4-tetrahydro-2-phenylthiochromeno[4,3-c]pyrazole (5) with 1M17 protein

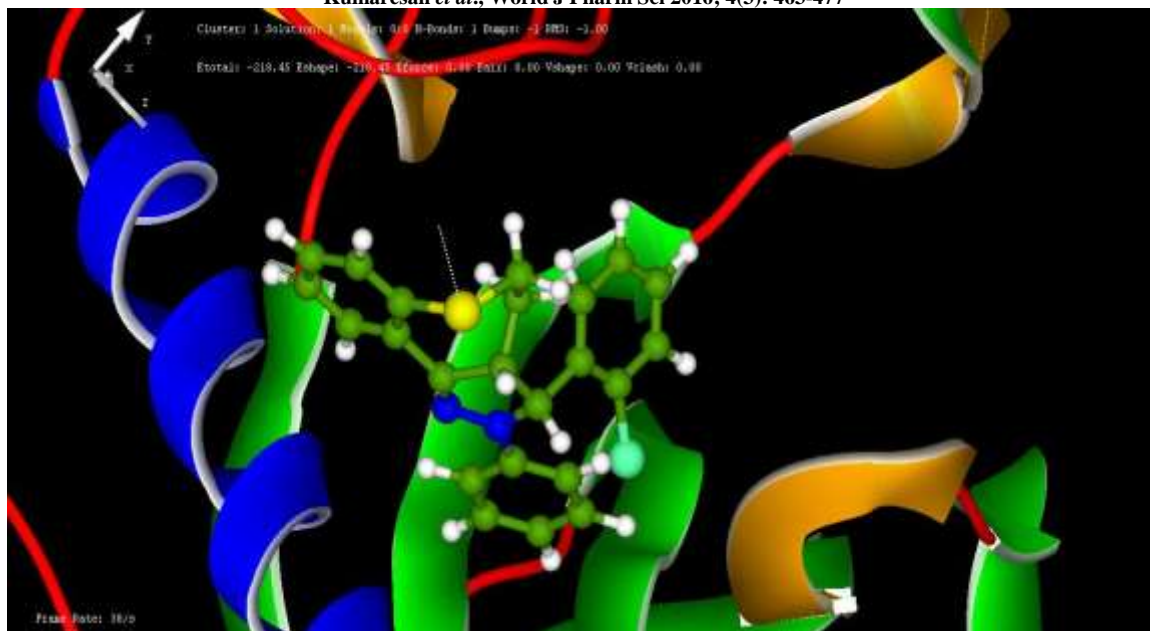


Fig. 3. Docking pose of 3-(4-chlorophenyl)-2-phenyl-3,3a,4,5-tetrahydro-2H-[1]benzothiepine[5,4-c]pyrazole (6) with 1M17 protein

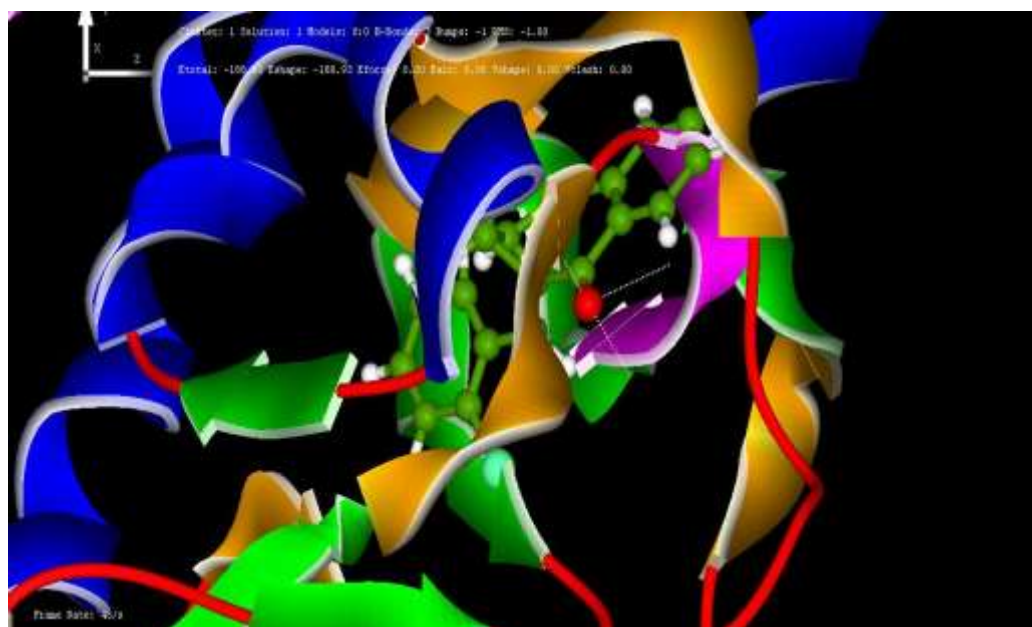


Fig. 4. Docking pose of 3-(2-chlorophenyl)-2,3,3a,4-tetrahydro-2-phenylthiochromeno[4,3-c]pyrazole (9) with 1M17 protein

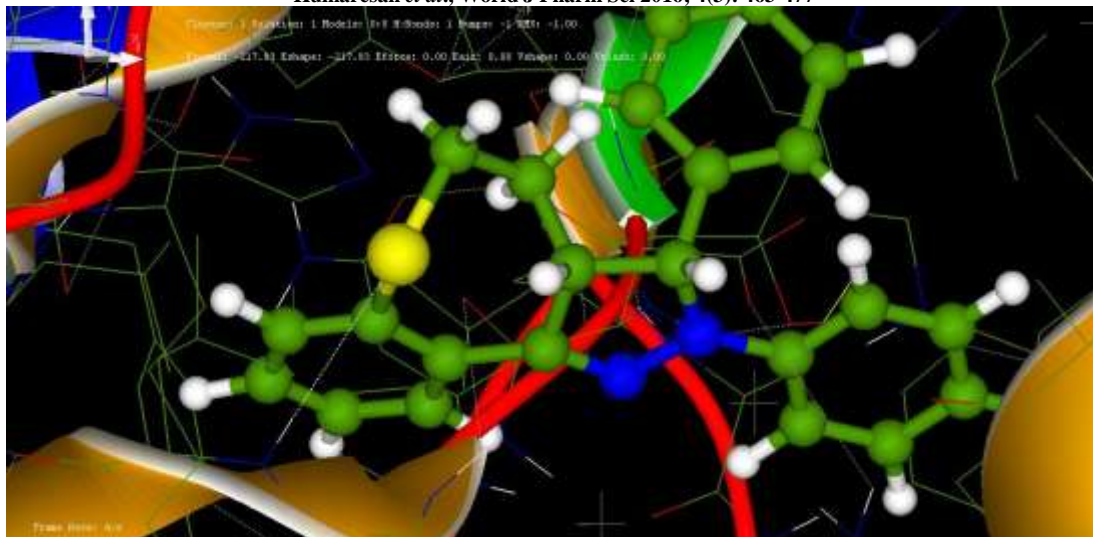


Fig. 5. Docking pose of 3-(2-chlorophenyl)-2-phenyl-3,3a,4,5-tetrahydro-2H-[1]benzothiepine[5,4-c]pyrazole (10) with 1M17 protein

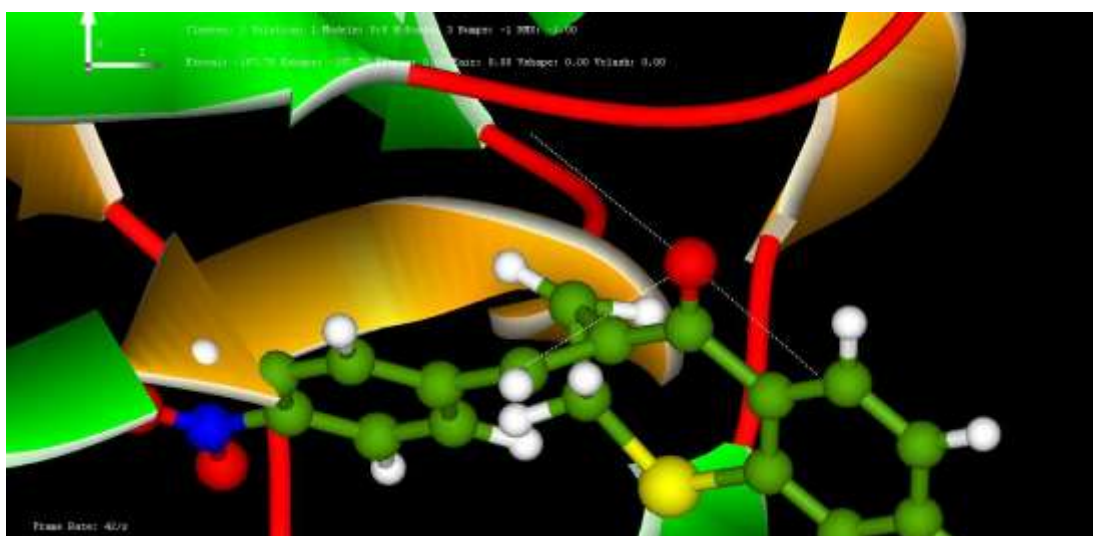


Fig. 6. Docking pose of 3-(4-nitrophenyl)-2,3,3a,4-tetrahydro-2-phenylthiochromeno[4,3-c]pyrazole (13) with 1M17 protein

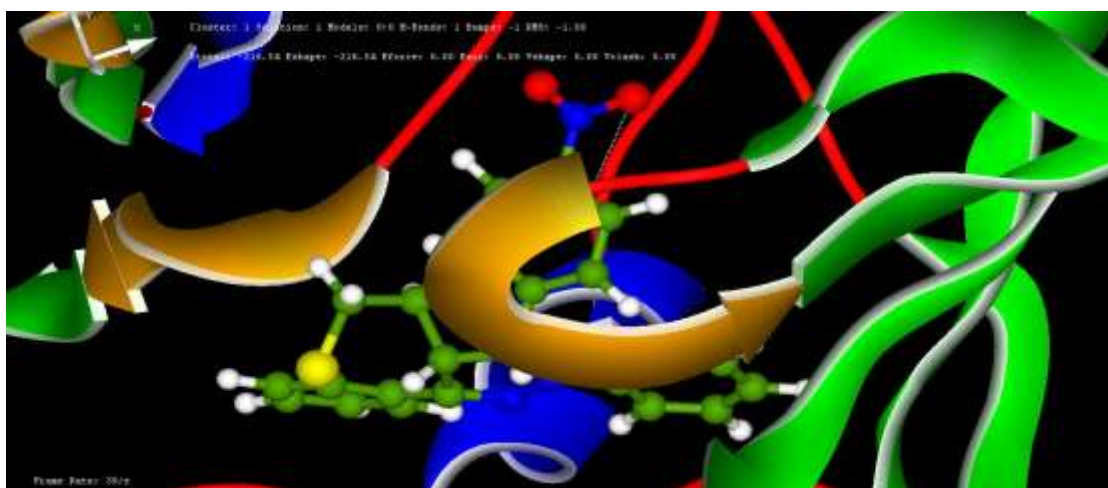


Fig. 7. Docking pose of 3-(4-nitrophenyl)-2-phenyl-3,3a,4,5-tetrahydro-2H-[1]benzothiepine[5,4-c]pyrazole (14) with 1M17 protein

Several derivatives containing 4-substituted phenylaminopyrazolo core have shown good affinity for enzyme binding site and led to new models of kinase inhibitors based on 1M17 protein [29]. Thus docking calculations were carried out on 1M17-REPLICATION protein model (Fig. 1). Essential hydrogen atoms, Kollman united atom type charges and rescue parameters were added with the aid of AutoDock Tools [30]. The estimated free energy of binding and the interacting surface of the compounds **5**, **6**, **9**, **10**, **13**, and **14** are given in Table 1.

From the docking analysis, the surface area of compound **6** is found to be the largest (986.423 Å²) in this series. Compound **6** has the lowest binding energy (-218.45 Kcal/mol) as compared to that of other pyrazole derivatives. This suggests that the designed pyrazole derivative **6** is a moderate promoter of 1M17 protein. VAL43, ALA47, and PRO79 are the interacting residues with minimum binding energy for compound **6**. Table 1 reveals that the benzothiepine derivatives **6**, **10**, and **14** possess lower binding energies compared to the thiochroman derivatives.

Table 1. Docking results for compounds 5, 6, 9, 10, 13, and 14.

Compound	Est. binding energy (Kcal/mol)	Est. inhibition constant, KI (μM)	Interacting surface Å ²	Interacting Residues
5	-189.78	19.94	875.421	VAL43, ALA47, PRO79
6	-218.45	18.51	986.423	VAL43, ALA47, PRO79
9	-188.93	24.86	04.36	ASN46, ASP73, PRO79
10	-217.83	23.24	763.428	ASN46, ASP73, PRO79
13	-187.78	30.12	608.631	VAL43, ALA47, PRO79
14	-216.54	28.62	654.821	VAL43, ALA47, PRO79

DFT Studies on compounds 5, 6, 9, 10, 13, and 14: Information on the molecular properties could be obtained from DFT studies. The B3LYP/3-21G (d) method has been successfully used to predict the geometry and electronic structure of a molecule [31]. All calculations were accomplished using Gaussian 09 software [32]. Gas phase geometry optimizations of **5**, **6**, **9**, **10**, **13**, and **14** were performed at the Density Functional Theory [DFT/B3LYP-3-21G (d)] level [33].

Gas phase geometrical parameters of the optimized structures at the DFT/3-21G (d) level are listed in Table 2. In total, we have investigated the electronic structures of the compounds **5**, **6**, **9**, **10**, **13**, and **14** using the DFT method. Figs. 8, 9, 10, 11, 12, and 13 represent the optimized structures of the pyrazole derivatives **5**, **6**, **9**, **10**, **13**, and **14** respectively.

The binding ability of the molecule increases with increasing HOMO and decreasing LUMO energy values. Thus, the lower the value of E_{LUMO}, the most probable it is that the molecule would accept electrons. Figs. 8-13 reveal the HOMO and LUMO

of pyrazole derivatives **5**, **6**, **9**, **10**, **13**, and **14** respectively. Moreover, the gap between the HOMO and LUMO energy levels (ΔE) of the molecule is an important parameter that determines the reactivity of the molecule. As ΔE decreases (most especially for the cationic species), the reactivity of the molecule increases leading to a decrease in the stability of the molecule. Compound **6** has the lowest energy gap and least stability and compound **13** has the highest energy gap and more stability.

Absolute hardness, η, and softness, σ, are important properties to measure the molecular stability and reactivity. A hard molecule has a large energy gap and a soft molecule has a small energy gap. Soft molecules are more reactive than hard ones because they could easily offer electrons to an acceptor. For the simplest transfer of electrons, absorption could occur at the part of the molecule where σ has the highest magnitude whereas η has the lowest [34]. The nucleophilicity, ω, measures the electrophilic power of a molecule. It has been reported that the lower the value of χ, the lower the capacity of the molecule to donate electrons [35].

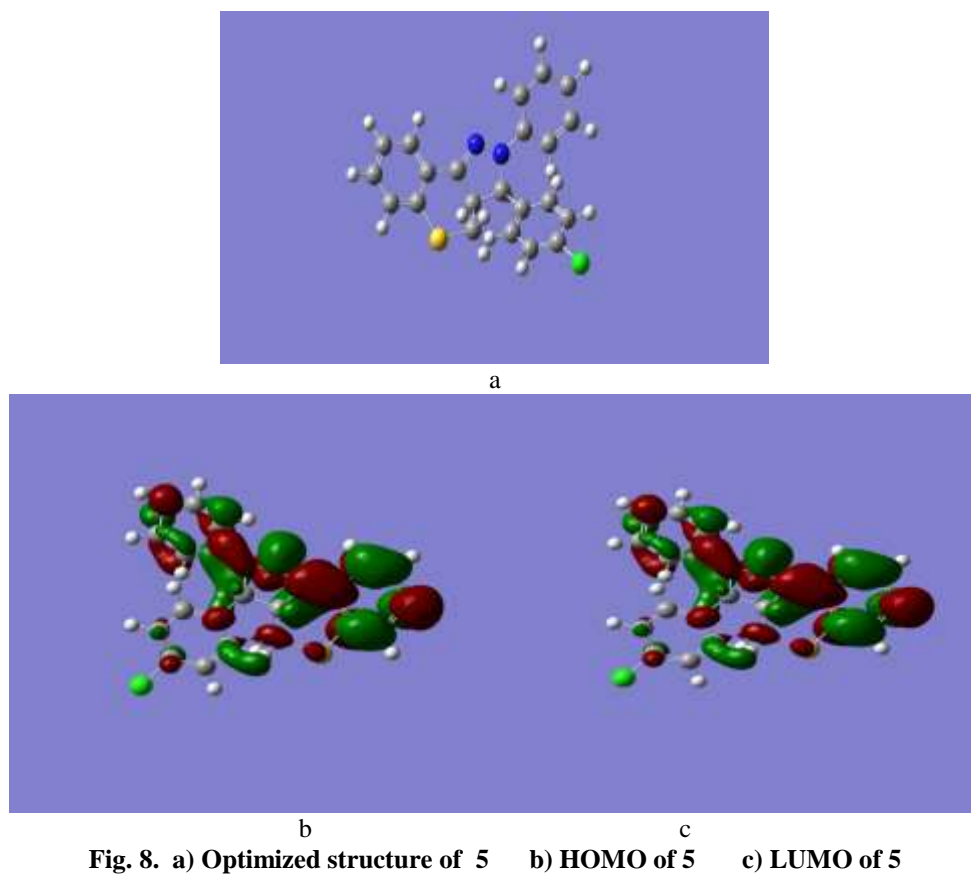


Fig. 8. a) Optimized structure of 5 b) HOMO of 5 c) LUMO of 5

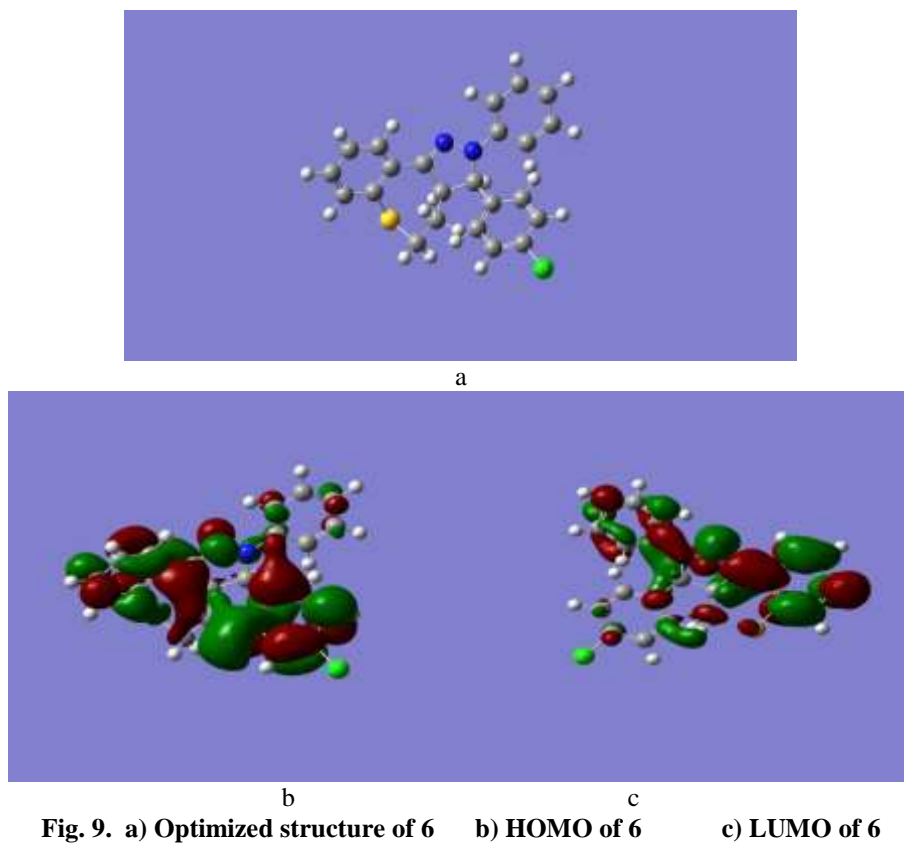
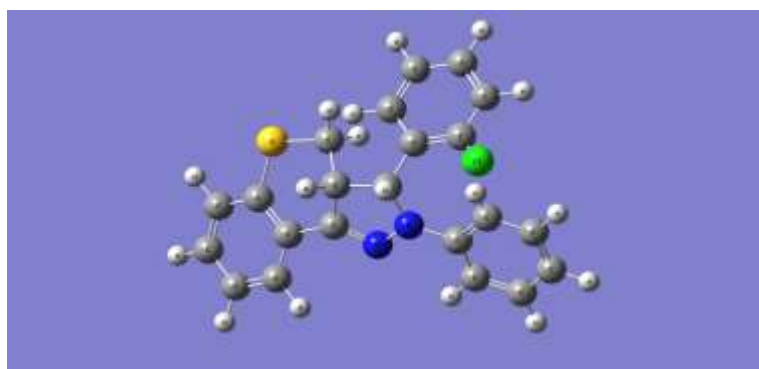
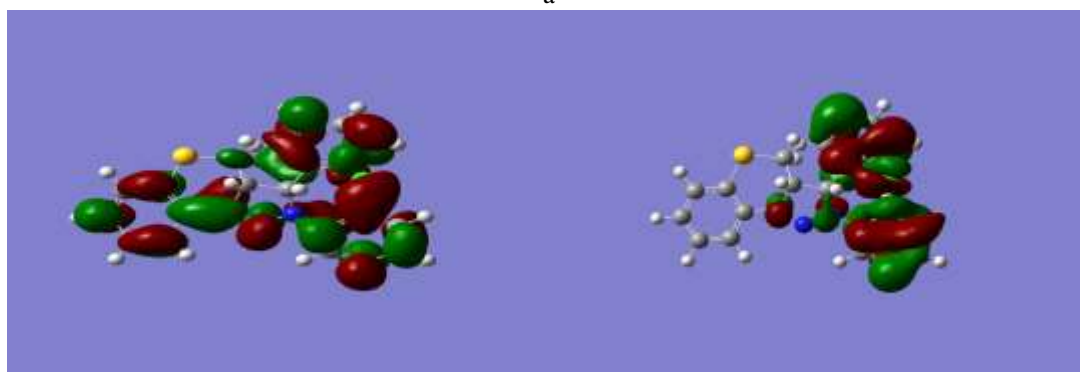


Fig. 9. a) Optimized structure of 6 b) HOMO of 6 c) LUMO of 6



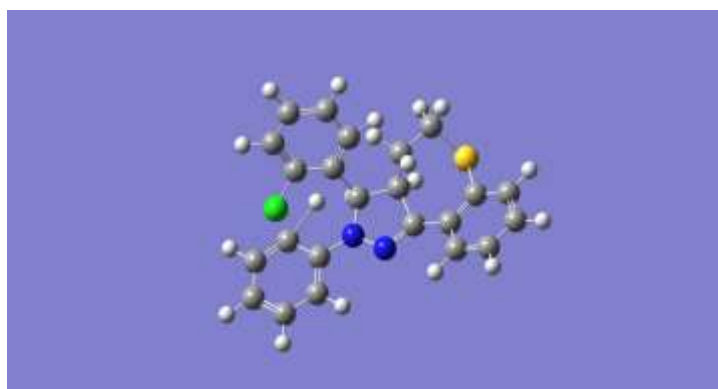
a



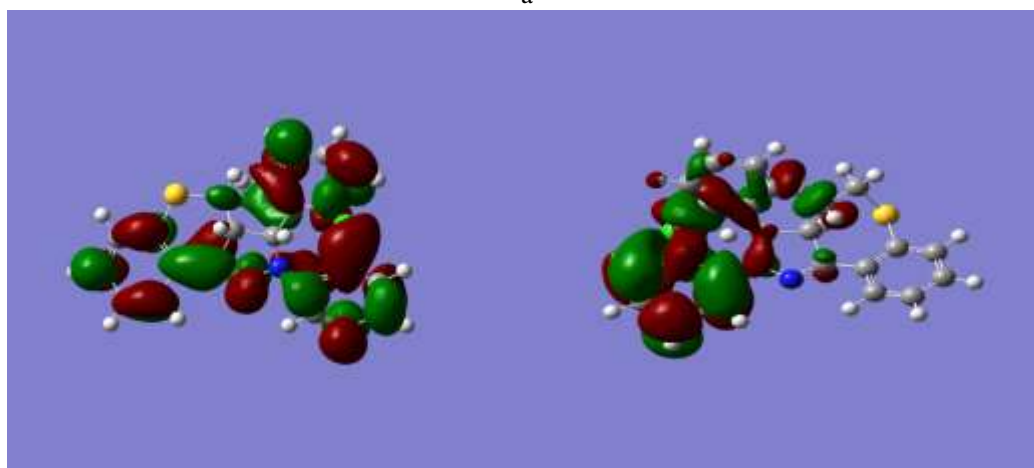
b

c

Fig. 10. a) Optimized structure of 9 b) HOMO of 9 c) LUMO of 9



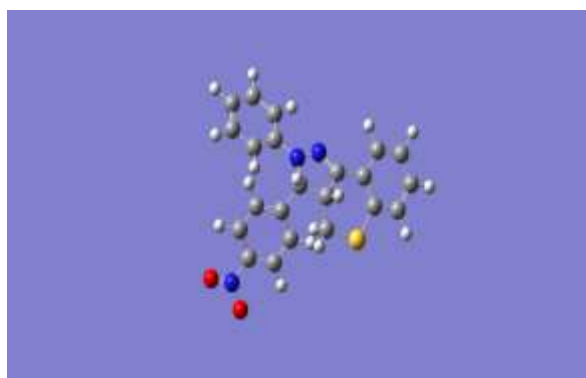
a



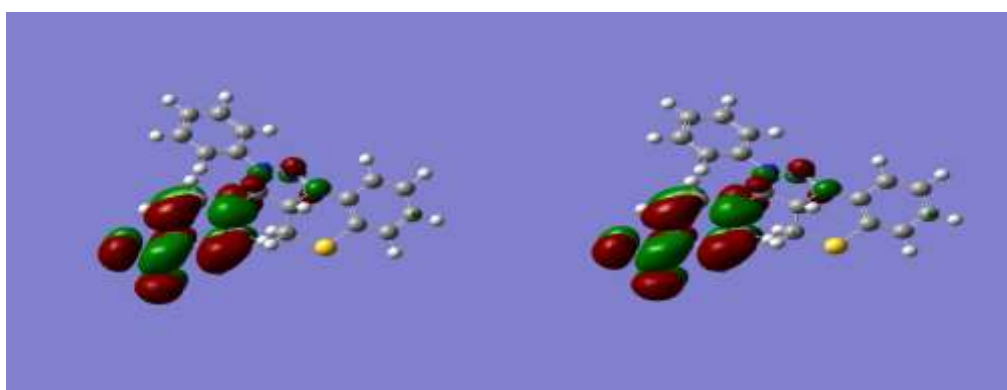
b

c

Fig. 11. a) Optimized structure of 10 b) HOMO of 10 c) LUMO of 10



a



b

c

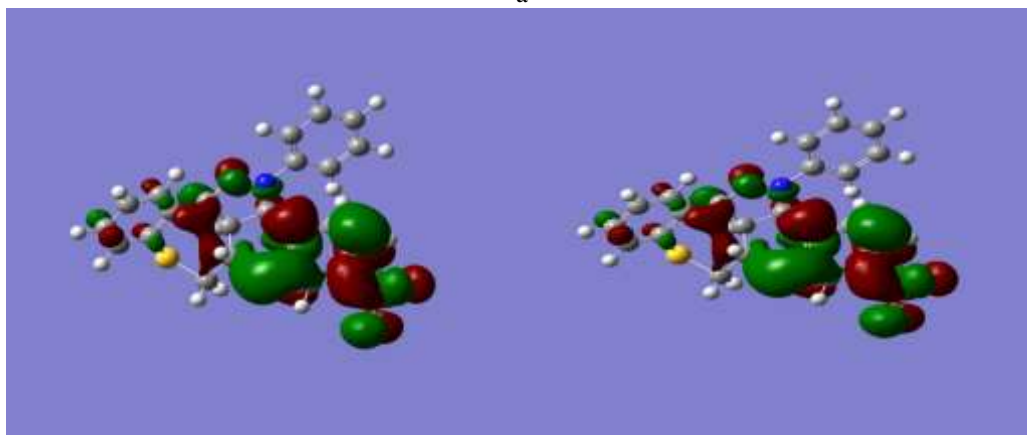
Fig. 12. a) Optimized structure of 13

b) HOMO of 13

c) LUMO of 13



a



b

c

Fig. 13. a) Optimized structure of 14

b) HOMO of 14

c) LUMO of 14

Kumaresan *et al.*, World J Pharm Sci 2016; 4(3): 463-477
Table 2. DFT results of compounds 5, 6, 9, 10, 13, and 14.

Compound	HOMO (eV)	LUMO (eV)	Energy gap (ΔE) (eV)	IP (eV)	EA (eV)	χ (eV)	μ (eV)	η (eV)	σ (eV)	ω (eV)
5	-0.14931	0.07485	0.22416	0.14931	-0.07485	0.037230	-0.03723	0.112080	8.922198	0.006183
6	-0.13724	0.06383	0.20107	0.13724	-0.06383	0.036705	-0.03671	0.100535	9.946785	0.006700
9	-0.16029	0.08507	0.24536	0.16029	-0.08507	0.037610	-0.03761	0.122680	8.151288	0.005765
10	-0.14504	0.07837	0.22341	0.14504	-0.07837	0.033335	-0.03334	0.111705	8.952151	0.004974
13	-0.22781	0.07474	0.30254	0.2278	-0.07474	0.076530	-0.07653	0.151270	6.610696	0.019359
14	-0.24693	0.05196	0.29889	0.24693	-0.05196	0.097485	-0.09749	0.149445	6.691425	0.031795

P = ionization potential; EA= electron affinity; χ = electronegativity; μ = electrochemical potential; η = hardness; σ = softness; ω = nucleophilicity

Table 3. Inhibition zone (mm) of compounds 5, 6, 9, 10, 13, and 14.

Compound	Zone of inhibition (mm)							
	Bacteria					Fungi		
	Gram-positive bacteria		Gram-negative bacteria			<i>Candida albicans</i>	<i>Aspergillus flavus</i>	<i>Aspergillus niger</i>
	<i>Staphylococcus aureus</i>	<i>Streptococcus pneumoniae</i>	<i>Klebsiella pneumoniae</i>	<i>Pseudomonas aeruginosa</i>	<i>Escherichia coli</i>			
5	10-13	25-28	09-12	24-27	14-17	26-29	12-15	07-10
6	11-14	26-29	10-13	26-29	17-19	27-30	14-17	08-11
9	08-11	23-25	07-10	22-25	12-15	25-28	10-13	09-09
10	07-10	26-29	08-11	23-26	13-16	26-29	11-14	10-13
13	16-19	13-16	11-14	14-17	16-19	13-16	10-13	19-22
14	16-19	12-15	12-15	15-18	17-20	14-17	12-15	20-23
Amikacin (Standard)	15-18	19-22	14-17	18-21	18-21	NT	NT	NT
Clotrimazole (Standard)	NT	NT	NT	NT	NT	24-27	17-20	21-24

NT- Not Tested

Table 2 shows that compound **6** has the lowest energy gap (ΔE , 0.20107 eV), lowest hardness (0.100535 eV), highest softness (9.946785 eV), and moderate nucleophilicity (0.036705 eV). The experimentally observed potent activity (Table 3 and Table 4) of compound **6** correlates better with the theoretical results obtained from DFT studies (Table 2).

Antimicrobial evaluation: All the six newly synthesized compounds **5**, **6**, **9**, **10**, **13**, and **14** were evaluated for their *in vitro* antibacterial activity against *Staphylococcus aureus*, and *Streptococcus pneumoniae*, as examples of Gram-positive bacteria and *Klebsiella pneumoniae*, *Pseudomonas aeruginosa*, and *Escherichia coli* as examples of Gram-negative bacteria. They were also evaluated for their *in vitro* antifungal potential against *Candida albicans*, *Aspergillus flavus*, and *Aspergillus niger* fungal strains. Agar-diffusion method was used for the determination of the preliminary antibacterial- and antifungal activity. Amikacin, and clotrimazole were used as reference drugs. For each tested compound, the results were recorded as the average diameter of inhibition zones (IZ) of bacterial- or fungal growth around the discs in mm³ (Table 3).

The results depicted in Table 3 revealed that most of the tested compounds displayed variable inhibitory effects on the growth of the tested bacterial strains, and also against antifungal strains. It would also be noticed that the chloro-substituted compounds (**5**, **6**, **9**, and **10**) exhibited better antimicrobial potentials than the nitro-substituted compounds (**13** and **14**). In this view, 3-(4-chlorophenyl)-2-phenyl-3,3a,4,5-tetrahydro-2H-[1]benzothiepine[5,4-c]pyrazole (**6**) was found to exhibit higher activity (26-29 mm, 23-26 mm, and 27-30 mm) than that of amikacin (19-22 mm and 18-21 mm), and clotrimazole (24-27 mm) against *Streptococcus pneumoniae* and *Pseudomonas aeruginosa*, and *Candida albicans*. Regarding the nitro-substituted pyrazole derivatives **13** and **14**, a comparable antimicrobial activity against *Staphylococcus aureus*, *Escherichia coli*, and *Aspergillus niger* was noticed.

In vitro antituberculosis activity: Recently Hadda *et al* have reported the synthesis and evaluation of the bioactivity of spirothiochromanone (STC) derivatives against *Trypanosoma cruzi* [36]. These

authors have described the importance of spirothiochromanone (STC)-pharmacophore sites for the potent antituberculosis activity. This prompted us to screen all the compounds synthesized by us for their *in vitro* antituberculosis activity against MTB (*H₃₇Rv*). The primary screening was carried out by agar-dilution method using two-fold dilution techniques. Isoniazid (INH) was used as a standard drug. The chloro-substituted pyrazole derivatives displayed better antituberculosis activity compared to their nitro-substituted counterparts. The observed data on the antituberculosis activity of the title compounds and the standard drug are given in Table 4. All compounds were found to be active with minimum inhibitory concentrations of 6.9-8.5 μ M. The chloro-substituted pyrazole derivative **6** showed good inhibitory activity against MTB at MIC 6.9 μ M (Table 4).

Table 4. Antituberculosis activity of compounds **5**, **6**, **9**, **10**, **13**, and **14**.

Compound	Antituberculosis activity MIC (μ M)
5	7.2
6	6.9
9	8.1
10	8.0
13	8.5
14	8.4
INH (standard)	8.6

DNA cleavage: The DNA cleavage (*E. coli*) potential of the titled compounds for was investigated using agarose gel electrophoresis method. In the gel electrophoresis, the changes are manifested by the change in the intensity of each band assigned to a particular form of DNA. The results (Fig. 14) indicate that all these tricyclic pyrazole derivatives can interact with *E. coli* DNA in the presence of H₂O₂. Chloro-substituted pyrazole derivatives (**5**, **6**, **9**, and **10**) can cleave DNA completely compared to other systems. As a result, it can be said that the ability of these compounds for the DNA cleavage may be considered as a major reason for the inhibitory effect of them on the growth of the pathogenic organisms.

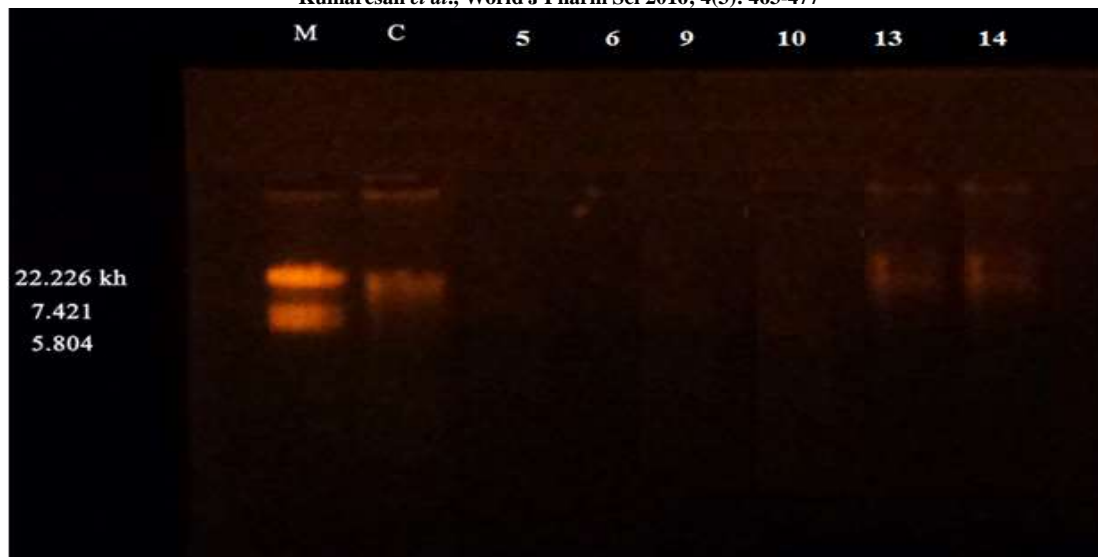


Fig.14 Gel electrophoresis pattern of compounds **5**, **6**, **9**, **10**, **13**, and **14** showing the effect on *E.coli* DNA. Lane M: DNA marker. Lane C: untreated DNA.

Conclusion

Six pyrazole derivatives (**5**, **6**, **9**, **10**, **13**, and **14**) have been synthesized from the Claisen-Schmidt condensation products **3**, **4**, **7**, **8**, **11**, and **12** respectively. All the pyrazole derivatives have been characterized by spectral techniques. Antimicrobial and antituberculosis studies for the new pyrazole derivatives have also been studied. Compound **6** showed the highest antimicrobial- and antituberculosis activity. Chloro-substituted pyrazole derivatives (**5**, **6**, **9**, and **10**) have shown a complete DNA cleavage compared to the nitro derivatives. The docking patterns for the six pyrazoles **5**, **6**, **9**, **10**, **13**, and **14** with *IM17*-Replication protein have been studied. Compound **6** has a lower binding energy (-218.45 Kcal/mol) as compared to other derivatives. DFT calculations

were performed using Gaussian 09 software. Compound **6** has the lowest energy gap (ΔE , 0.20107 eV), lowest hardness (0.100535 eV), highest softness (9.946785 eV), and lower nucleophilicity (0.036705eV). These results agree with the experimental observations that **6** shows better bioactivity.

Acknowledgements

We are thankful to the UGC, New Delhi for the financial support to do this work. One of the authors (P. P) thanks CDRI-Lucknow for the $^1\text{H-NMR}$, $^{13}\text{C-NMR}$ and mass spectral data and Malar Microbiological Laboratory, Tirunelveli, Tamilnadu for antimicrobial studies. Prof. Dr. K. Veluraja is profusely thanked for his assistance in the theoretical studies.

REFERENCES

1. Fomun ZT, Ifeadike PN. Heterocycles of biological importance. Part 2. Novel synthesis and pharmacological evaluation of 5-amino-3-alkyl-1-(2-pyridyl)pyrazoles and 5-amino-3-phenyl-1-(2-pyridyl)pyrazole from allenic or acetylenic nitriles and 2-hydrazinopyridine, *J. Heterocycl. Chem.*, 1985, 22(6), 1611.
2. Ronald EO. Biologically active pyrazoles, *J. Pharm. Sci.*, 1968, 57(4), 537.
3. Turan-Zitouni G, Sivaci M, Kilic FS, Erol K. Synthesis of some triazolyl-antipyrene derivatives and investigation of analgesic activity, *Eur. J. Med. Chem.*, 2001, 36, 685.
4. Hutchinson I, Jennings SS, Vishnuvajjala BR, Westwell AD, Stevens MFG. Antitumor Benzothiazoles. 16.1 Synthesis and Pharmaceutical Properties of Antitumor 2-(4-Aminophenyl)benzothiazole Amino Acid Prodrugs, *J. Med.Chem.*, 2002, 45, 744.
5. Quiroga J, Hernandez P, Insuasaty BR, Abonia R, Cobo J, Control of the reaction between 2-aminobenzothiazoles and Mannich bases. Synthesis of pyrido[2,1-b][1,3]benzothiazoles versus [1,3]benzothiazolo[2,3-b]quinazolines, *J. Chem. Soc., Perkin Trans.*, 2002, 1, 555.
6. Bonde CG, Gaikwad N, Synthesis and preliminary evaluation of some pyrazine containing thiazolines and thiazolidinones as antimicrobial agents, *J. Bioorg. Med. Chem.*, 2004, 12, 2151.
7. Kucukguzel SG, Oruc EE, Rolls S, Sahin F, Ozbek A, Synthesis, characterisation and biological activity of novel 4-thiazolidinones, 1,3,4-oxadiazoles and some related compounds, *Eur. J. Med. Chem.*, 2002, 37, 197.
8. Cesure N, Cesur Z, Ergenc N, Uzun M, Kiraz M, Kasimoglu O, Kaya D. Synthesis and Antifungal Activity of Some 2-Aryl-3-substituted 4-Thiazolidinones. Synthese und antimykotische Aktivität einiger 2-Aryl-3-substituierter 4-Thiazolidinone, *Arch. Pharm.*, 1994, 271.

9. Bhatt JJ, Shah BR, Shah HP, Trivedi PB. Synthesis of Anti HIV, Anticancer and Antitubercular 4-oxothiazolidines, 2-imino-4-oxo-thiazolidines and their 5-arylidene derivatives, *Ind. J. Chem.*, 1994, 33B, 189.
10. Kinugawa J, Ochiai M, Yamamoto H, Matsumura C. Studies on Fungicides. VII. Synthesis and Antifungal Activity of Some Pyrazole Derivatives, *Chem. Pharm. Bull.*, 1964, 12, 182.
11. Oliva A, Molinari A, Zuniga F, Ponce P. Studies on the Liquid-Liquid Extraction of Nickel(II), Zinc(II), Cadmium(II), Mercury(II) and Lead(II) with 1-Phenyl-3-hydroxy-4-dodecyldithiocarbonylate-5-pyrazolone, *Microchim. Acta*, 2002, 140, 201.
12. Herrag L, Chetouani A, Elkadiri S, Hammouti B, Aouniti A. Pyrazole Derivatives as Corrosion Inhibitors for Steel in Hydrochloric Acid, *Port. Electrochim. Acta*, 2008, 26, 211.
13. Holzer W, Pocher I. Synthesis and ¹³C NMR study of some *N*-substituted 4-iodo- and 3,4-diiodopyrazoles, *J. Heterocycl. Chem.*, 1995, 32, 189.
14. Haddad N, Baron J. Novel application of the palladium-catalyzed *N*-arylation of hydrazones to a versatile new synthesis of pyrazoles, *Tetrahedron Lett.*, 2002, 43, 2171.
15. Ram VJ, Singha UK, Guru PY. Chemotherapeutic agents XI: synthesis of pyrimidines and azolopyrimidines as leishmanicides, *Eur. J. Med. Chem.*, 1990, 25, 533.
16. Jyothilkumari KR, Rajasekharan KN. Synthesis of Some New Pyrazolo³, 4-d-pyrimidine Derivatives and their Antibacterial Activity, *J. Indian Chem. Soc.*, 1991, 68, 578.
17. Zani F, Vicini P. Antimicrobial Activity of Some 1,2-Benzisothiazoles Having a Benzenesulfonamide Moiety, *Arch. Pharm.*, 1998, 331, 219.
18. Ballesteros B, Santos L. A reinvestigation of the molecular structures, vibrations and rotation of methyl group in *o*-methylaniline in *S*₀ and *S*₁ states studied by laser induced fluorescence spectroscopy and ab initio calculations, *Spectrochim. Acta.*, 2002, 58A, 1069.
19. Andreani A, Granaola M, Leoni A, Morigi R, Rambaldi M. Synthesis and antitubercular activity of imidazo[2,1-*b*]thiazoles, *Eur. J. Med. Chem.*, 2001, 36, 743.
20. Kini SG, Bhat AR, Bryant B, Williamson JS, Dayan FE. Synthesis, antitubercular activity and docking study of novel cyclicazole substituted diphenyl ether derivatives, *Eur. J. Med. Chem.*, 2009, 44, 492. **20a.** Mason S, Morize I, Menard PR, Cheney DL, Hulme C, Labaudiniere RF, New 4-Point Pharmacophore Method for Molecular Similarity and Diversity Applications: Overview of the Method and Applications, Including a Novel Approach to the Design of Combinatorial Libraries Containing Privileged Substructures, *J. Med. Chem.*, 1999, 42, 3251.
21. Palanisamy P, Kumaresan S, Analogues of *N*,1-diphenyl-4,5-dihydro-1*H*-[1]benzothiepine[5,4-*c*]pyrazole-3-carboxamide and *N*,1-diphenyl-4,5-dihydro-1*H*-[1]benzothiepine[5,4-*c*]pyrazole-3-carboxamide-6,6-dioxide: syntheses, characterization, antimicrobial, antituberculosis, and antitumor activity, *RSC Advances*, 2013, 3(14), 4704.
22. Kumaresan S, Palanisamy P. □ Analogues of *N*, 1-Diphenyl 1-4,5-Dihydro-1 H- [1] benzothiepine [5,4-*c*] pyrazole-3 -carboxamide and of *N*, 1-Diphenyl 1-4,5-Dihydro-1 H-[1] benzothiepine [5,4-*c*] pyrazole-3-carboxamide: Syntheses Characterization Antituberculosis-, Antimicrobial and Antitumor Activity, *Int. J. Adv. Phar.Res.*, 2013, 4(2), 1402.
23. Kumaresan S, Ramadass SR. Polyhetero polycyclic ring systems: part xxi: synthesis of *d*-homo-6,11,15-trithia-1,3,5(10),8,13-gonapentaen-17a-one, *Phosphorus and Sulfur*, 1984, 19, 295.
24. Morris GM, Goodsell DS, Halliday RS, Huey R, Hart WE, Below RK, Olson AR. Automated docking using a Lamarckian genetic algorithm and an empirical binding free energy function, *J. Comput Chem.*, 1998, 19, 1639.
25. Anand P, Singh B, Singh N, A review on coumarins as acetylcholinesterase inhibitors for Alzheimer's disease, *Bioorg Med Chem.*, 2012, 20(3), 1175.
26. Halgren TA, Merck molecular force field. I. Basis, form, scope, parameterization, and performance of MMFF94, *J. Comput Chem.*, 1998, 17(5-6), 490.
27. Morris GM, Huey R, Lindstrom W, Sanner MF, Belew RK, Goodsell DS, Olson AJ, AutoDock4 and AutoDockTools4: Automated docking with selective receptor flexibility, *J Comput Chem.*, 2009, 30(16), 2785-2791
28. Thomas A. Halgren, Merck molecular force field. II. MMFF94 van der Waals and electrostatic parameters for intermolecular interactions, *J. Comput Chem.*, 1998, 17 (5-6), 490.
29. Burchat AF, Calderwood J, Frieman MM, Hirst C, Rafferty P, Ritter KS, Akinen S, Pyrazolo[3,4-*d*]pyrimidines containing an extended 3-substituent as potent inhibitors of Lck — a selectivity insight, *Bioorg. Med. Chem. Lett.*, 2002, 12, 1687.
30. Solis W, Minimization by Random Search Techniques, *Mathematics of Operations Research*, 1981, 6(1), 19.
31. Zandler ME, Souza FD, calculations to describe geometry, spectral and electrochemical properties of molecular and supramolecular porphyrin–fullerene conjugates, *Comptes Rendus ChimieChimie C.R.*, 2006, 9, 960.
32. Becke AD. Densityfunctional thermochemistry. III. The role of exact exchange, *J. Chem. Phys.*, 1993, 98, 5648.
33. Rajeev S, Kumar D, Bhoop S, Singh VK, Ranjana S. Molecular structure, vibrational spectroscopic and HOMO, LUMO studies of *S*-2-picoly-*l*-*N*-(2-acetylpyrrole) dithiocarbamate Schiff base by Quantum Chemical investigations, *Res J Chem Sci.*, 2013, 3(2), 79.
34. Parr RG, Pearson RG. Absolute hardness: companion parameter to absolute electronegativity, *J. Am. Chem. Soc.*, 1983, 105, 7512.
35. Parr RG, Szentpaly LV, Liu S. Electrophilicity Index, *J. Am. Chem. Soc.*, 1999, 121, 1922.
36. Hadda TB, Kerbal A, Bennani B, Houari GA, Daoudi M, Leite ACL, Masand VH, Jawarkar RH, Charrouf Z, Molecular drug design, synthesis and pharmacophore site identification of spiroheterocyclic compounds: *Trypanosoma cruzi* inhibiting studies, *Med. Chem. Res.*, 2013, 22, 57.
37. Morris. GM, Goodsell DS, Automated docking using a Lamarckian genetic algorithm and an empirical binding free energy function, *J Comput. Chem.*, 1998, 19 (14), 1639.
38. Gasteiger J, Engel T. Graph Theory in Chemistry. Ovidiu Ivanciuc. Sealy Center for Structural Biology and Molecular Biophysics, Cheminformatics –Wiley-VCH, 2003.
39. Monga PK, Sharma D, Dubey A, Comparative Study of Microwave and Conventional Synthesis and Pharmacological activity of Coumarins : A Review, *J Chem Pharm Res.*, 2012, 4(1), 822.
40. Sambrook J, Fritsch EF, Maniatis T, Molecular Cloning. A Laboratory Manual. 2nd Edn. Cold Spring Harbor Laboratory, Cold Spring Harbor, New York. (1989) 1626.